Article

Facile Synthesis for Ordered Mesoporous -Aluminas with High Thermal Stability

Quan Yuan, An-Xiang Yin, Chen Luo, Ling-Dong Sun, Ya-Wen Zhang, Wen-Tao Duan, Hai-Chao Liu, and Chun-Hua Yan

J. Am. Chem. Soc., **2008**, 130 (11), 3465-3472 • DOI: 10.1021/ja0764308

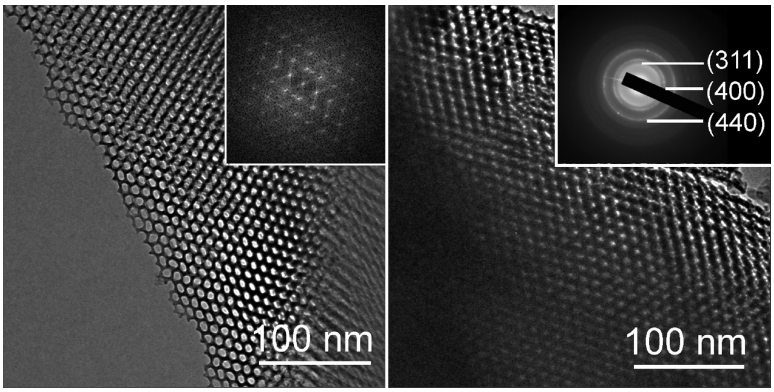

More About This Article

Additional resources and features associated with this article are available within the HTML version:

- Supporting Information
- Links to the 2 articles that cite this article, as of the time of this article download
- Access to high resolution figures
- Links to articles and content related to this article
- Copyright permission to reproduce figures and/or text from this article

View the Full Text HTML

J|A|C|S
ARTICLES
Published on Web 02/20/2008

Facile Synthesis for Ordered Mesoporous γ-Aluminas with High Thermal Stability

Quan Yuan, An-Xiang Yin, Chen Luo, Ling-Dong Sun, Ya-Wen Zhang, Wen-Tao Duan, Hai-Chao Liu,* and Chun-Hua Yan*

Beijing National Laboratory for Molecular Sciences, State Key Laboratory of Rare Earth Materials Chemistry and Applications and the PKU-HKU Joint Laboratory in Rare Earth Materials and Bioinorganic Chemistry, State Key Laboratory for Structural Chemistry of Stable and Unstable Species, Peking University, Beijing 100871, China

Received August 27, 2007; E-mail: yan@pku.edu.cn, hcliu@pku.edu.cn

Abstract: The facile synthesis of highly ordered mesoporous aluminas with high thermal stability and tunable pore sizes is systematically investigated. The general synthesis strategy is based on a sol−gel process associated with nonionic block copolymer as templates in ethanol solvent. Small-angle XRD, TEM, and nitrogen adsorption and desorption results show that these mesoporous aluminas possess a highly ordered 2D hexagonal mesostructure, which is resistant to high temperature up to 1000 °C. Ordered mesoporous structures with tunable pore sizes are obtained with various precursors, different acids as pH adjustors, and different block copolymers as templates. These mesoporous aluminas have large surface areas (ca. 400 m^2/g), pore volumes (ca. 0.70 cm^3/g), and narrow pore-size distributions. The influence of the complexation ability of anions and hydro-carboxylic acid, acid volatility, and other important synthesis conditions are discussed in detail. Utilizing this simple strategy, we also obtained partly ordered mesoporous alumina with hydrous aluminum nitrate as the precursor. FTIR pyridine adsorption measurements indicate that a large amount of Lewis acid sites exist in these mesoporous aluminas. These materials are expected to be good candidates in catalysis due to the uniform pore structures, large surface areas, tunable pore sizes, and large amounts of surface Lewis acid sites. Loaded with ruthenium, the representative mesoporous alumina exhibits reactant size selectivity in hydrogenation of acetone, D-glucose, and D-(+)-cellobiose as a test reaction, indicating the potential applications in shape-selective catalysis.

Introduction

Since the ordered mesoporous silica material was first reported in 1992,[1] the interest in this research field has expanded all over the world due to the potential applications of these materials in catalysis and in other realms of chemistry. Compared to silica, alumina is more popular in catalysis area for its broad applications as industrial catalysts and catalyst supports employed in petroleum refinement, automobile emission control, and others.[2] With the characteristics of mesoporous materials, such as highly uniform channels, large surface area, narrow pore-size distribution, tunable pore sizes over a wide range, and so on, alumina with a mesostructure should possess much more excellent properties.

Nonsiliceous materials with ordered mesoporosity are commonly prepared through the sol−gel process with surfactants as structure-directing agents (SDAs) or by utilizing the nanocasting method with silica or carbon materials as hard templates. However, the synthesis of ordered and thermal stable mesoporous alumina represents a much more complex problem[3] due to its susceptibility for hydrolysis as well as to the phase transitions accompanying the thermal breakdown of the ordered structure. Although particular attentions have been devoted to the synthesis of mesoporous aluminas, unfortunately disordered structures with amorphous walls were fabricated in most cases.[4−9] According to previous reports,[10−12] the hydrolysis behavior of alumina is very complicated and strongly affected by acid, water, temperature, relative humidity, and other factors, giving rise to rather strict synthetic conditions for ordered mesoporous aluminas.[13] Pinnavaia et al.[14] obtained pseudo lamellar mesostructured γ-alumina with crystalline framework walls.

(1) (a) Kresge, C. T.; Leonowicz, M. E.; Roth, W. J.; Vartuli. J. C.; Beck, J. S. *Nature* **1992**, *359*, 710. (b) Beck, J. S.; Vartuli. J. C, Roth, W. J.; Leonowicz, M. E.; Kresge, C. T.; Schmitt, K. D.; Chu, C. T-W.; Olson, D. H.; Sheppard, E. W.; McCullen, S. B.; Higgins, J. B.; Schlenkert, J. L. *J. Am. Chem. Soc.* **1992**, *114*, 10834.
(2) (a) Tung, S. E.; Mcininch, E. *J. Catal.* **1964**, *3*, 229. (b) Topsoe, H.; Clausen, B.S.; Massoth, F.E. *Hydrotreating Catalysis*; Springer: Berlin, 1996; p 310.
(3) Čejka, J. *Appl. Catal., A* **2003**, *254*, 327.
(4) Bagshaw, S. A.; Prouzet, E.; Pinnavaia, T. J. *Science* **1995**, *269*, 1242.
(5) Vaudry, F.; Khodabandeh, S.; Davis, M. E. *Chem. Mater.* **1996**. *8*. 1451.
(6) Yada, M.; Ohya, M.; Machida, M.; Kijima, T. *Chem. Commun.* **1998**, 1941.
(7) Cabrera, S.; Haskouri, J. E.; Alamo, J.; Beltrán, A.; Betrán, D.; Mendioroz, S.; Marcos, M. D.; Amorós, P. *Adv. Mater.* **1999**, *11*, 379.
(8) Bagshaw, S. A.; Pinnavaia, T. J. *Angew. Chem., Int. Ed.* **1996**, *35*, 1102.
(9) Zhang, W.; Pinnavaia, T. J. *Chem. Commun.* **1998**, 1185.
(10) Baes, C. F; Mesmer, R. E. *The Hydrolysis of Cations*; Wiley: New York, 1976; p 112.
(11) Swaddle, T. W.; Rosenqvist, J.; Yu, P.; Bylaska, E.; Phillips, B. L.; Casey, W. H. *Science* **2005**, *308*, 1450.
(12) Casey, W. H. *Chem. Rev.* **2006**, *106*, 1.
(13) Niesz, K.; Yang, P.; Somorjai, G. A. *Chem. Commun.* **2005**, 1986.
(14) (a) Zhang, Z. R.; Hicks, R. W.; Pauly, T. R.; Pinnavaia, T. J. *J. Am. Chem. Soc.* **2002**, *124*, 1592. (b) Zhang, Z. R.; Pinnavaia T. J. *J. Am. Chem. Soc.* **2002**, *124*, 12294.

Employing aluminum tri-*tert*-butoxide as the main inorganic precursor and anhydrous aluminum chloride as the pH adjustor and hydrolysis−condensation controller, Zhao et al.[15] fabricated partly ordered mesoporous alumina. Somorjai et al.[13] first reported the synthesis of ordered mesoporous alumina with amorphous walls through a sol−gel route under strict control of the hydrolysis procedure as well as the condensation of reagents. By utilizing the dip-coating method, Sanchez et al. synthesized ordered nanocrystalline γ-Al_2O_3 films with contracted *fcc* mesoporosity.[16] Following the above work, Grosso, D. et al. improved the synthesis procedure and fabricated ordered nanocrystalline mesoporous γ-alumina powders by aerosol generation of the initial solution using an ITS atomizer.[17] After treatment at 700 °C γ-alumina was obtained and it could be stable up to 900 °C. Recently, Zhang and co-workers[18] developed an ordered crystalline mesoporous alumina molecular sieve with CMK-3 as hard template, which presented a new route to obtain ordered mesoporous alumina. However, this synthesis procedure requires multiple steps and is time-consuming. From the viewpoint of synthesis, it is still a significant challenge to obtain γ-alumina with highly ordered mesostructures via a one-step, convenient, and economic approach. Moreover, the thermal stability and catalysis properties of ordered mesoporous alumina have not been studied in detail yet.

Herein, we present an easily accessible, reproducible, and high-throughput method to synthesize highly ordered mesoporous aluminas with amorphous and/or crystalline γ-phase framework walls through a simple sol−gel route with block copolymers as the soft templates. With this strategy, a series of ordered mesoporous aluminas with 2D hexagonal structure are readily obtained, and partly ordered mesoporous alumina is also fabricated with hydrous aluminum nitrate as the precursor. More important, these mesoporous aluminas exhibit a high thermal stability up to 1000 °C, possess high surface areas, tunable pore sizes, and large amount of surface Lewis acid sites, and show a reactant size selectivity in hydrogenation of acetone, D-glucose, and D-(+)-cellobiose.

Experimental Section

Chemicals. Pluronic P123 (M_{av} = 5800, $EO_{20}PO_{70}EO_{20}$), Pluronic F127 (M_{av} = 12 600, $EO_{106}PO_{70}EO_{106}$), and Pluronic F68 (M_{av} = 8400, $EO_{77}PO_{29}EO_{77}$) were purchased from Aldrich and Sigma-Aldrich. Aluminum iso-propoxide, $Al(NO_3)_3{\cdot}9H_2O$, HNO_3, HCl, citric acid, and DL-malic acid were purchased from Beijing Chemical Reagents. Aluminum tri-*tert*-butoxide was purchased from Acros Corp. Tartaric acid was purchased from Sinopharm Chemical Reagent Co., Ltd. Commercial γ-alumina was purchased from Alfa Aesar. All other chemicals were used as received.

Synthesis. In a typical synthesis, 0.8−1.0 g of Pluronic P123 was dissolved in 20 mL of ethanol at room temperature. Then 1.4−1.6 mL of 67 wt % nitric acid (or 1.4−1.6 mL of 37 wt % hydrochloric acid plus 0.5 g citric acid) and 2.04 g (10 mmol) of aluminum iso-propoxide were added into the above solution with vigorous stirring. The mixture was covered with PE film, stirred at room temperature for about 5 h, and then put into a 60 °C drying oven to undergo the solvent evaporation process. After 2 days of aging, the solution became a light-yellow solid (when hydrochloric acid and citric acid were used, white solids were obtained). Calcination was carried out by slowly increasing temperature from room temperature to 400 °C (1 °C min^{-1} ramping rate) and by heating at 400 °C for 4 h in air. High-temperature treatment was carried out in air for 1 h with a temperature ramp of 10 °C min^{-1}.

Table 1. Synthesis Conditions and Obtained Ordered Mesoporous Aluminas

sample	alumina precursor	template	acid	d_{100} (nm) 400 °C	d_{100} (nm) 900 °C
Al-1	$Al(OPr^i)_3$	Pluronic P123	HNO_3	9.0	9.0
Al-2	$Al(OPr^i)_3$	Pluronic P123	$HCl + C_6H_8O_7{\cdot}H_2O$	9.0	8.3
Al-3	$Al(OPr^i)_3$	Pluronic P123	$HCl + C_4H_6O_6$	7.6	8.0
Al-4	$Al(OPr^i)_3$	Pluronic P123	$HCl + C_4H_6O_5$	10.7	8.6
Al-5	$Al(OPr^i)_3$	Pluronic F127	HNO_3	10.8	10.0
Al-6	$Al(OPr^i)_3$	Pluronic F127	$HCl + C_6H_8O_7{\cdot}H_2O$	9.8	9.2
Al-7	$Al(OPr^i)_3$	Pluronic F127	$HCl + C_4H_6O_6$	8.0	10.5
Al-8	$Al(OPr^i)_3$	Pluronic F127	$HCl + C_4H_6O_5$	10.8	9.4
Al-9	$Al(OBu^s)_3$	Pluronic P123	HNO_3	11.0	9.6
Al-10	$Al(OBu^s)_3$	Pluronic P123	$HCl + C_6H_8O_7{\cdot}H_2O$	8.2	8.3
Al-11	$Al(NO_3)_3{\cdot}9H_2O$	Pluronic P123	$C_6H_8O_7{\cdot}H_2O$	7.9	7.0

Catalyst Preparation. Supported ruthenium catalysts containing 2 wt % ruthenium were prepared by incipient wetness impregnation of as-synthesized mesoporous Al_2O_3 and for comparison, commercial Al_2O_3 (Alfa Aesar) with an aqueous solution of $Ru(NO)(NO_3)$ (Alfa Aesar) (denoted hereinafter as ruthenium/meso-Al_2O_3 and ruthenium/commerical-Al_2O_3, respectively) at 25 °C for 12 h. Impregnated samples were dried in ambient air at 120 °C for 24 h and then reduced under flowing H_2/N_2 (10/90 v/v) at 350 °C for 6 h.

Characterization. PXRD patterns were recorded on a Rigaku D/MAX-2000 diffractometer (Japan) using Cu Kα radiation (λ = 1.5406 Å). TEM were taken on the Hitachi H-9000 NAR transmission electron microscope under a working voltage of 300 kV. The nitrogen adsorption and desorption isotherms at 78.3 K were measured using an ASAP 2010 analyzer (Micromeritics Co. Ltd.). FTIR spectra were recorded on a Nicolet Magna-IR 750 spectrometer equipped with a Nic-Plan Microscope. ^{27}Al MAS NMR spectra were recorded on a Varian Unity Inova spectrometer operating at 78.155 MHz (0.3 μs as a pulse width), an acquisition time of 0.02 s and a pulse delay of 1 s. The acidities of the samples were determined by the pyridine adsorption technique. Pyridine FTIR spectra were recorded with a BIO-RAD FTS-3000 FTIR spectrometer.

Catalytic hydrogenation reactions of acetone, D-glucose, and D-(+)-cellobiose were carried out in a Teflon-lined stainless steel autoclave (150 mL) typically at 120 °C and 4 MPa H_2 using deionized water (50 mL) as a solvent. Reactants and products were analyzed by high-performance liquid chromatography (HPLC) (Agilent 1100).

Results and Discussion

Table 1 summarizes the ordered mesoporous aluminas synthesized with different aluminum precursors, surfactants, and acids. Ordered mesoporous aluminas are achieved with whichever aluminum iso-propoxide, aluminum sec-butoxide, or hydrous aluminum nitrate is used as the precursor. Different acids are added as the pH adjustors for the hydrolysis of aluminum precursors, and the results demonstrate that it is flexible to obtain the ordered mesostructure in a wide range of acidity and water content. For example, sample Al-1 (synthesized with aluminum iso-propoxide as the precursor, nitric acid as the acid adjustor, and Pluronic P123 as the surfactant) is prepared with the appropriate molar ratio of HNO_3 to $Al(OPr^i)_3$ in the range of 2.0−2.4. Compared with the synthesis of ordered mesoporous alumina reported by Somorjai et al.,[13] the ratio of HNO_3 to Al-

(15) Tian, B. Z.; Yang, H. F.; Liu, X. Y.; Xie, S. H.; Yu, C. Z.; Fan, J.; Tu, B.; Zhao, D. Y. *Chem. Commun.* **2002**, 1824.
(16) Kuemmel, M.; Grosso, D.; Boissière, C.; Smarsly, B.; Brezesinski, T.; Albouy, P. A.; Amenitsch, H.; Sanchez, C. *Angew. Chem., Int. Ed.* **2005**, *44*, 4589.
(17) Boissière, C.; Nicole, L.; Gervais, C.; Babonneau, F.; Antonietti, M.; Amenitsch, H.; Sanchez, C.; Grosso, D. *Chem. Mater.* **2006**, *18*, 5238.
(18) Liu, Q.; Wang, A. Q.; Wang, X. D.; Zhang, T. *Chem. Mater.* **2006**, *18*, 5153.

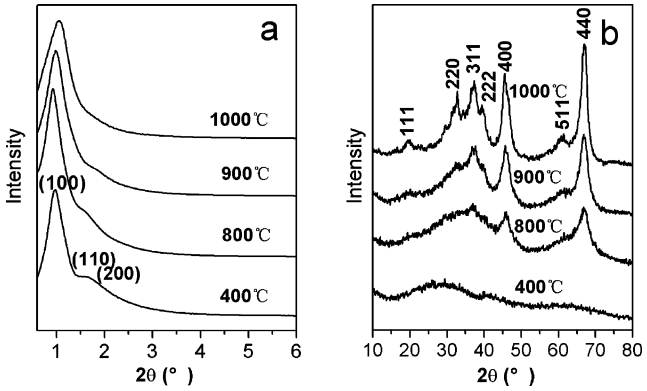

Figure 1. (a) Small- and (b) wide-angle XRD patterns of Al-1 calcined at different temperatures.

$(OPr^i)_3$ does not have to be strictly fixed at a specific composition.

Evidence for the formation of mesostructures is provided by small-angle X-ray diffraction (XRD) patterns shown in part a of Figure 1. The sample Al-1 calcined at 400 °C shows a very strong diffraction peak around 1.0° and one weak peak around 1.7°, which, according to the TEM observation, can be attributed to *p*6*mm* hexagonal symmetry. A good mesoscopic order is reflected even after calcination at 800, 900, and 1000 °C, respectively, indicating a high thermal stability of the mesoporous structure. Part b of Figure 1 shows the wide-angle XRD patterns of Al-1 calcined at different temperatures. Calcination at 400 °C gives rise to the mesostructure with amorphous wall, and then the amorphous wall is converted to γ-Al_2O_3 phase (JCPDS Card No. 10−0425) after further treatment at a temperature of 800 °C. The combination of the small- and wide-angle XRD data convince us that the ordered mesoporous γ-alumina with crystalline walls are prepared at 800−1000 °C. After being calcined at 1100 °C, no diffraction peak is observed in the low-angle range (Figure S1 in the Supporting Information), demonstrating that the mesoporous structure has collapsed; whereas diffraction peaks of α-Al_2O_3 phase (JCPDS Card No. 11−0661) phase appear in the wide-angle XRD pattern (Figure S1 in the Supporting Information).

TEM images of Al-1 annealed at 400 °C are displayed in parts a and b of Figure 2 with the corresponding fast Fourier transform (FFT) patterns. The highly ordered hexagonal arrangement of pores along [001] direction and the alignment of cylindrical pores along [110] direction are observed. With the samples prepared in different batches, more images (Figure S2 in the Supporting Information) display the similar well-ordered pore network observed for the sample Al-1 calcined at 400 °C and show the consistence between the same sample viewed from different areas and between the samples prepared in different batches. The TEM images (parts c and d of Figure 2) also confirm to us that the ordered mesoporous structures are retained after 900 °C treatment. The selective area electron diffraction (SAED) pattern (the insert in part c of Figure 2) of the ordered mesostructure domains indicates that the mesoporous wall is crystalline with γ-Al_2O_3 phase. Additional proof for the crystallinity of the framework walls is given by high-resolution TEM investigations (part e of Figure 2), which reveals the existence of several crystalline nanoparticles with well-defined lattice planes. Ordered mesostructure domains are also observed for

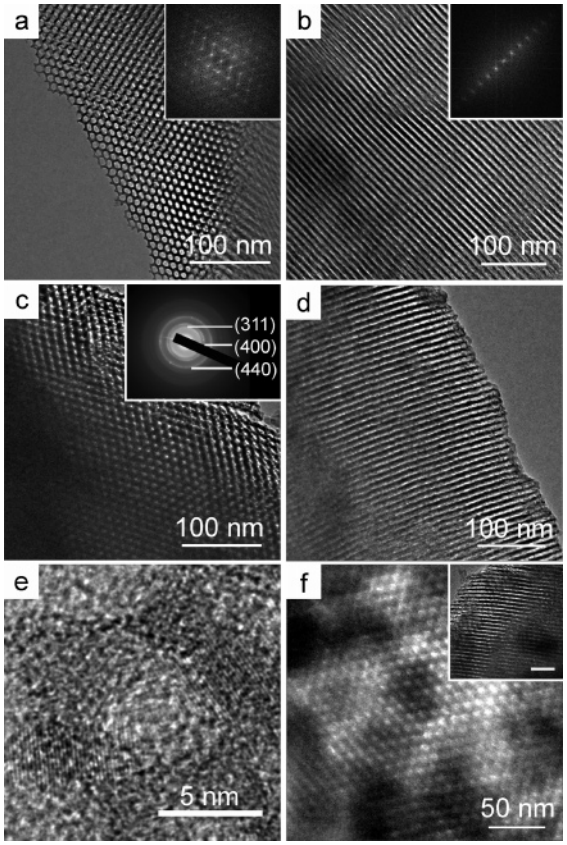

Figure 2. TEM images (a) and (b) of Al-1 calcined at 400 °C viewed along [001] and [110] orientations (FFT diffractogram inset), TEM images (c) and (d) of Al-1 calcined at 900 °C viewed along [001] and [110] orientations (the insert in c is corresponding SAED pattern), (e) HRTEM image of Al-1 calcined at 900 °C, (f) TEM image of Al-1 calcined at 1000 °C viewed along [001] orientation (the inset is TEM image viewed along [110] orientation). The bars are 50 nm for insets.

the sample calcined at 1000 °C (part f of Figure 2), further proving the high thermal stability of the mesostructure.

The nitrogen adsorption−desorption isotherms (Figure 3) of Al-1 treated at different temperatures all yield type IV curves with H1-shaped hysteresis loops, suggesting their uniform cylindrical pores. Al-1 treated at 400 °C has a large BET surface area of 434 m^2/g and a pore volume of 0.80 cm^3/g (Table S1 in the Supporting Information). When transformed into γ-alumina, it still exhibits a BET surface area of 226, 220, and 116 m^2/g at 800, 900, and 1000 °C, respectively. Narrow pore-size distributions (4−6 nm) are maintained though the diameter decreases as the calcination temperature increases. The large surface areas and narrow pore-size distributions combined with excellent thermal stability enhance the potential applications of these ordered mesoporous aluminas in catalysis.

Hydrochloric acid is added in the system to replace nitric acid. Unfortunately, only a broad peak is observed in small angle XRD pattern, denoting a short range ordered mesostructure (part a of Figure 4). If small amounts of hydro-carboxylic acids like citric acid (CA), tartaric acid, and DL-malic acid are introduced into this system, long range ordered mesostructures are obtained according to the small-angle XRD patterns (part a of Figure 4). This is confirmed by TEM observations (parts a, c, and d of Figure 5), which clearly show the ordered hexagonally packed cylindrical mesopores. These mesoporous structures are resistant to the temperature up to 900 °C (part b of Figure 4 and part b

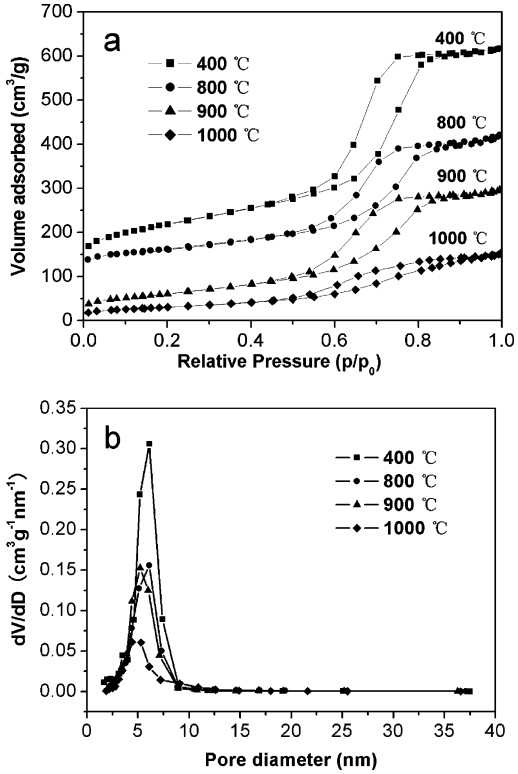

Figure 3. (a) Nitrogen adsorption−desorption isotherms and (b) pore-size distribution curves (deduced from the desorption branches) of Al-1. For clarity, the isotherms for 900 and 1000 °C products in (a) are offset along the *y* axis by 100 and 100 cm^3/g, respectively.

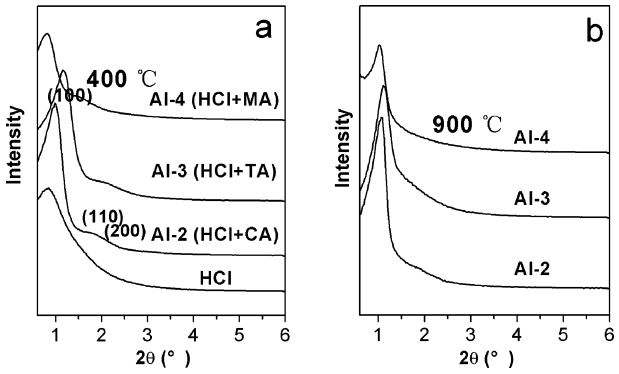

Figure 4. Small-angle XRD patterns of mesoporous aluminas synthesized using HCl plus HCAs as pH adjustors at (a) 400 and (b) 900 °C.

of Figure 5). The N_2 adsorpion−desorption isotherms for both Al-2 (synthesized with aluminum iso-propoxide as the precursor, HCl plus CA as the acid adjustor, and Pluronic P123 as the surfactant) treated at 400 and 900 °C (Figure S3 in the Supporting Information) show typical type IV curves with a distinct condensation step at a p/p_0 range of 0.5−0.8, suggesting uniform mesopores (ca. 4 nm). BET analysis for Al-2 treated at 400 °C gives a surface area of about 450 m^2/g and a pore volume of 0.57 cm^3/g (Table S1 in the Supporting Information). Transformed to γ-alumina, it still exhibits a BET surface area of 256 m^2/g and a pore volume of 0.45 cm^3/g.

In the present work, a series of highly ordered mesoporous aluminas with 2D hexagonal structures are fabricated with different acids as pH adjustors. According to the "liquid crystal templating" mechanism for the formation of mesoporous structure proposed by Beck et al.,[1] the ultimate liquid crystalline phases may be related to the ionic strength, counterion polarizability, surfactant concentration, counterion charge, and other factors. Stucky et al.[19] proposed the cooperative organization mechanism based on the charge density matching at the organic−inorganic interface. Regarding metal-based materials, four different mechanisms, charge matching,[20,21] ligand-assisted templating,[22,23] ion exchange/scaffolding,[24] and modulation of the hybrid interface,[25] have been proposed according to the experiment results of different spectroscopical characterizations such as NMR, fluorescence or UV−vis absorption. On the basis of our results and former models, in our case, the complexation abilities of surfactants, ions, and hydro-carboxylic acids play important roles in the mesophase formation. Alkylene oxide segments can form crown-ether-type complexes with inorganic ions including multivalent metal species through coordination bonds.[26] Accompanied by hydrolysis and condensation, the metal species associate with the hydrophilic poly(ethyleneoxide) moieties of copolymer molecules via electrostatics and van der Waals forces to guide mesostructure formation.[27] Balanced Coulombic, hydrogen bonding, and van der Waals interactions with charge matching at interfaces provide an effective means of enhancing long-range periodic order. Zhao et al.[28] reported that the radius and charge of the anions such as Cl^-, I^-, and NO_3^- impose a great effect on the reaction rate and the assembly process of the silicate−surfactant mesophase. In our experi-

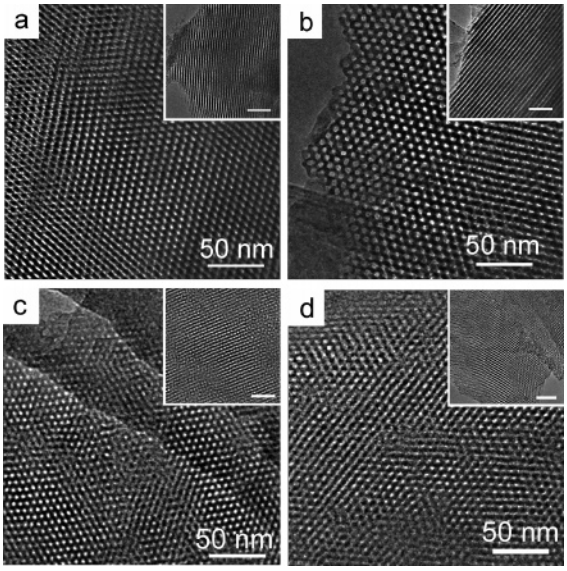

Figure 5. TEM images of (a) Al-2 (400 °C), (b) Al-2 (900 °C), (c) Al-3 (400 °C), and (d) Al-4 (400 °C). The bars are 50 nm for insets.

(19) Firouzi, A.; Kumar, D.; Bull, L. M.; Besier, T.; Sieger, P.; Huo, Q.; Walke, S. A.; Zasadzinski, J. A.; Glinka, C.; Nicol, J.; Margolese, D.; Stucky, G. D.; Chmelka, B. F. *Science* **1995**, *267*, 1138.
(20) (a) Huo, Q.; Margolese, D. I.; Ciesla, U.; Demuth, D. K.; Feng, P.; Gier, T. E.; Sieger, P.; Firouzi, A.; Chmelka, B. F.; Schüth, F.; Stucky, G. D. *Chem. Mater.* **1994**, *6*, 1176. (b) Huo, Q.; Margolese, D. I.; Ciesla, U.; Feng, P.; Gier, T. E.; Sieger, P.; Leon, R.; Petroff, P. M.; Schüth, F.; Stucky, G. D. *Nature* **1994**, *368*, 317.
(21) Luca, V.; Hook, J. M. *Chem. Mater.* **1997**, *9*, 2731.
(22) Ying, J. Y.; Mehnert, C. P.; Wong, M. S. *Angew. Chem., Int. Ed.* **1999**, *38*, 57.
(23) Antonelli, D. M.; Ying, J. Y. *Angew. Chem., Int. Ed.* **1996**, *35*, 426.
(24) Hudson, M. J.; Knowles, J. A. *J. Mater. Chem.* **1996**, *6*, 89.
(25) (a) Soler-Illia, G. J. A. A.; Sanchez, C. *New J. Chem.* **2000**, *24*, 493. (b) Soler-Illia, G. J. A. A.; Scolan, E.; Louis, A.; Albouy, P.-A.; Sanchez, C. *New J. Chem.* **2001**, *25*, 154.
(26) Bailey, F. E., Jr; Koleske, J. V. *Alkylene Oxides and Their Polymers*; Marcel Dekker: New York, 1990.
(27) Yang, P.; Zhao, D.; Margolese, I.; Chmelka, B. F.; Stucky, G. D. *Nature* **1998**, *396*, 152.
(28) Zhao, D. Y.; Huo, Q. S.; Feng, J. L.; Chmelka, B. F.; Stucky, G. D. *J. Am. Chem. Soc.* **1998**, *120*, 6024.

ments, NO_3^- does not strongly influence the self-assembly process because of its weak complexation ability. However, chloride ion can strongly coordinate with aluminum ions, and it might destroy the balance of the organic−inorganic interface and disturb the assembly process,[14b] leading to long-range disordered mesostructures. Hydro-carboxylic acids are good coordination agents for aluminum ions via monodentate or bridging bidentate modes.[29,30] Zhang et al.[31] have proposed that hydro-carboxylic acids can act as SDA in the formation of mesoporous γ-alumina via the coordination between the hydro-carboxylic acid and aluminum sites of aluminum oxohydroxide particulates. FTIR spectra of the pure citric acid as well as as-synthesized mesoporous alumina using hydrochloric acid plus citric acid as pH adjustors are presented in Figure S4 in the Supporting Information. For the pure CA, the absorption band positioned at 1724 cm^{-1} is ascribed to the υ(C═O) carbonyl stretching vibration of the free carboxylic acid (COOH) groups, whereas a C−O stretching vibration absorption band at 1380 cm^{-1} is assigned to the free carboxylate groups of CA moleclules.[32,33] The as-synthesized alumina sample with a CA/Al ratio of 0.10 exhibits a new absorption band at 1450 cm^{-1}, which is assigned to a C−O bond of increased single bond order due to the monodentate coordinated carboxylate groups that are bound with the aluminum atoms.[32] The absorption bands of both the free CA and the chelated CA exist in this as-synthesized alumina, indicating that not all of the three carboxylate groups of the CA are bonded to the surface of the alumina presursor.[33] If the CA/Al ratios are not lower than 0.15, the band at 1724 cm^{-1} disappears whereas the band of 1450 cm^{-1} remains. This trend suggests that the CA−Al complex is formed through the binding of the carboxylate groups to aluminum ions. It is believed that the complexation between carboxylic groups and aluminum ions takes place prior to hydrolysis−condensation of the inorganic precursors and is enhanced upon drying and thermal treatment. CA serves as an inhibitor for hydrolysis−condensation process of aluminum species through coordinating with one or two aluminum sites on very small clusters of AlOOH. In the case of alumina- or other metal-based (such as titanium, zirconium, and niobium) oxide mesostructures, acetylacetone was used as an inhibitor in neutral or slightly acidic medium in the presence of alkyl phosphate templates.[34−36] Triethanolamine was employed in strongly basic media as chelates in the synthesis of mesoporous alumina.[7] In the case with CA, the complexation interaction between HCA and alumina precursor is also observed. These HCAs are competitors against chloride ions, both of which coordinate with aluminum ions through the whole evaporation process. Meanwhile, HCA can interact with the block copolymers through hydrogen bonding and the van der Waals force, and then protect the aluminum ions at the organic−inorganic interface from being affected by chloride ions. Incidentally, corresponding small-angle XRD patterns (Figure S5 in the Supporting Information) display that ordered mesostructures can be obtained with the CA/Al^{3+} ratio in the range of 0.15 to 0.35, demonstrating that only appropriate chelation between HCAs and alumina precursors can lead to ordered assembly.

We assume that volatilization behavior of the acids is an important factor that should be taken into account. The reactivity of the alumina precursors can be efficiently regulated through various methods such as careful adjustment of the pH and dilution of solutions or the use of condensation inhibitors.[37] A subsequent slowing step is necessary to irreversibly freeze a half-condensed structure and hence avoids the fast formation of an inorganic network. Inorganic hydrolysis and condensation have to be controlled to fabricate a robust mesostructure instead of a hard solid. As for our synthesis, the starting solutions are relatively dilute, and the inorganic polymerization can be readily dominated by an acid, which is subsequently removed by evaporation. In the case of this system, as the volatility of HCl is higher than that of HNO_3, the acidity of the whole system added with HCl in evaporation process reduces more quickly and thus consequently influences the hydrolysis behavior of aluminum species and the self-assembly process. When non-volatile hydro-carboxylic acids are introduced, they act as sustained-release agents to maintain an acidic equilibrium environment for precursors. In the beginning, their effect is not obvious, whereas at the end of the evaporation process this effect becomes more important as hydro-carboxylic acids' concentration increase in the whole system.

Besides, the synthesis conditions, particularly the amount of water, pH, temperature, and relative humidity, have a great impact on the final mesophase. The water quantity has crucial effects on the formation kinetics of the condensed phase and on the chemical compatibility at the hybrid interface.[37] The fine-tuning of the water/precursor ratios should place the systems in the right position to obtain the desired mesostructure. Herein, a low water quantity is necessary. The species and dose of acid do directly determine not only the sort of cations that affect the self-assembly process through coordination interaction with the aluminum precursor but also the pH of the medium. A small amount of H^+ slows down the hydrolysis rate of the aluminum alkoxide, making the dissolution of the precursor molecules difficult in ethanol, whereas higher H^+ concentration results in uncontrollable fast hydrolysis of aluminum alkoxide. Therefore, the amount of H^+ is restricted to a relatively narrow range. At the same time, it is also necessary to control proper ambient factors, like temperature and relative humidity. The formation of a well-defined mesostructure depends critically on these factors, which controls two competitive processes: solvent evaporation and inorganic polymerization.[38] In our synthesis, high temperature and low relative humidity (<20%) are adopted by placing the reaction vessels in a drying oven with the temperature set at 60 °C. After evaporating for 2 days, the product has been totally condensed to a foam-like product without fluidity. Varying the evaporation time from 2 to 8 days, the same 2D hexagonal mesostructures are obtained, implying that it is the most stable mesostructure under this synthesis condition. Two days is a proper choice for the sake of synthesis efficiency.

(29) Motekaitis, R.; Martell, A. *Inorg. Chem.* **1984**, *23*, 18.
(30) Hidber, P. C.; Graule, T. J.; Gauckler, L. J. *J. Am. Ceram. Soc.* **1996**, *79*, 1857.
(31) Liu, Q.; Wang, A. Q.; Wang, X. D.; Zhang, T. *Microporous Mesoporous Mater.* **2006**, *92*, 10.
(32) Thornton, D. A. *Coord. Chem. Rev.* **1990**, *104*, 173.
(33) Hidber, P. C.; Graule, T. J.; Gauckler, L. J. *J. Am. Ceram. Soc.* **1996**, *79*, 1857.
(34) Antonelli, D. M.; Ying, J. Y. *Angew. Chem., Int. Ed. Engl.* **1995**, *34*, 2014.
(35) Putnam, R. L.; Nakagawa, N.; McGrath, K. M.; Yao, N.; Aksay, I. A.; Gruner, S. M.; Navrotsky, A. *Chem. Mater.* **1997**, *9*, 2690.
(36) Antonelli, D. M.; Nakahira, A.; Ying, J. Y. *Inorg. Chem.* **1996**, *35*, 3126.
(37) Soler-Illia, G. J. A. A.; Sanchez, C.; Lebeau, B.; Patarin, J. *Chem. Rev.* **2002**, *102*, 4093.
(38) Soler-Illia, G. J. A. A.; Louis, A.; Sanchez, C. *Chem. Mater.* **2002**, *14*, 750.

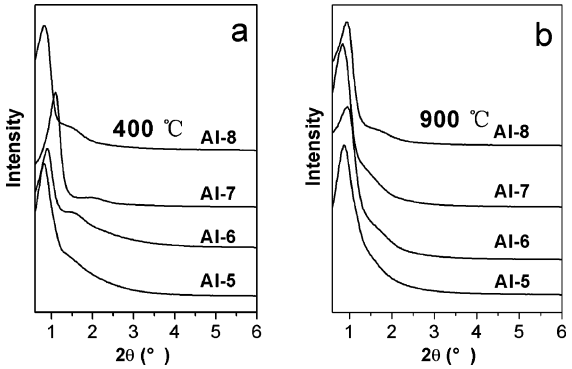

Figure 6. Small-angle XRD patterns of mesoporous aluminas using F127 as SDA calcined at (a) 400 and (b) 900 °C.

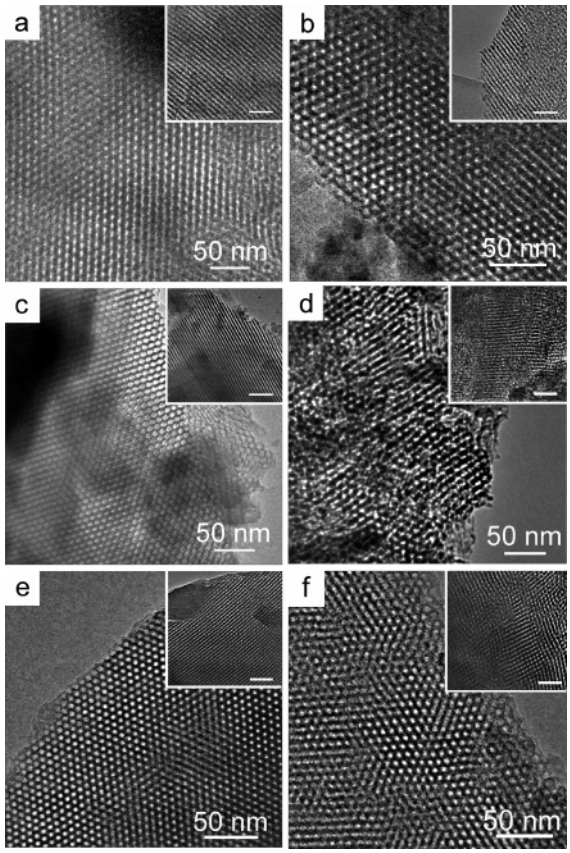

Figure 7. TEM images of mesoporous aluminas using F127 as SDA calcined at different temperatures (a) Al-5 (400 °C), (b) Al-5 (900 °C), (c) Al-6 (400 °C), (d) Al-6 (900 °C), (e) Al-7 (400 °C), and (f) Al-8 (400 °C). The bars are 50 nm for insets.

Ordered mesoporous aluminas are attained using different ethylene oxide-based surfactants via the same synthesis strategy. Poly(alkylene oxide) triblock copolymers like P123, F127(EO_{106}-$PO_{70}EO_{106}$), and F68($EO_{77}PO_{29}EO_{77}$) are used as SDAs. The surfactants with different EO/PO ratios and different molecular weights result in different structures and pore sizes. Under our synthesis conditions, with F68 as surfactant only a wormlike structure is prepared, whereas P123 and F127 are good SDAs to fabricate an ordered mesostructue. Small-angle XRD patterns (Figure 6) all indicate the ordered mesostructures with 2D hexagonal symmetry with F127 as SDA, which is further confirmed by TEM observations (Figure 7) showing the ordered mesoporous structures. Corresponding nitrogen adsorption−desorption isomers combined with pore-size distribution curves are displayed in Figure S6 in the Supporting Information.

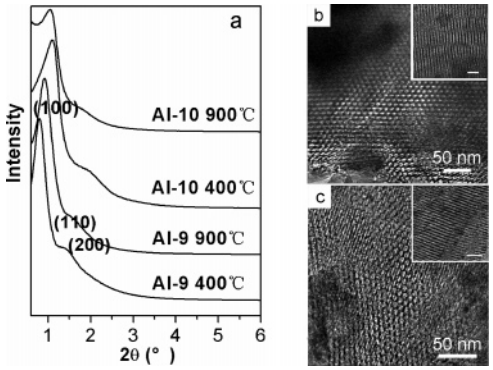

Figure 8. (a) Small-angle XRD patterns of mesoporous aluminas using $Al(OBu^s)_3$ as the precursor. TEM images of Al-9 calcined at (b) 400 and (c) 900 °C. The bars are 50 nm for insets.

Substituting aluminum tri-*tert*-butoxide for aluminum isopropoxide as the precursor, highly ordered mesoporous aluminas are also achieved (Figure 8). Nitrogen sorption measurements show a narrow pore-size distribution around about 4−7 nm (Figure S7 in the Supporting Information), BET surface area of 350−460 m^2/g, and pore volumes of 0.68−0.75 cm^3/g (Table S1 in the Supporting Information). After transformed into γ-alumina, they still exhibit BET surface areas of 190−210 m^2/g at 900 °C.

In particular, it is worthwhile to investigate the use of hydrous aluminum nitrate as the precursor because hydrous aluminum nitrate is cheaper and easily acquired. In previous reports[14,39] concerning the use of aluminum nitrate as the precursor, only short range ordered mesostructures were obtained as a result of the uncontrollable hydrolysis of aluminum nitrate. With citric acid as the acid adjustor, we have successfully synthesized ordered mesoporous alumina (Figure 9). Small-angle XRD pattern shows a sharp peak at 1.1° accompanied by a weak peak around 2.0°. Ordered domains with a 2D hexagonal mesophase are detected, whereas wormlike structures exist as well (parts b and c in Figure 9). It exhibits a lower BET surface area of about 250 m^2/g (Table S1 in the Supporting Information) but a narrower pore-size distribution (Figure S8 in the Supporting Information) than that produced by using aluminum alkoxide as the precursor. As the CA/Al^{3+} ratio varies from 0.4 to 0.9, the intensity of the (100) diffraction peak together with that of the second-order peak becomes weaker (Figure S9 in the Supporting Information). On the basis of these results, it is postulated that in this system the complexation ability of citric acid is a key feature in obtaining mesostructured phases.

The ^{27}Al MAS NMR spectra (part a of Figure 10) of Al-1 treated at 400 °C present three resonance signals at 70, 35, and 0 ppm. These bands are assigned to the central $\langle -1/2, 1/2 \rangle$ transition of the Al^{3+} ion in tetrahedral (AlO_4), pentahedral (AlO_5), and octahedral (AlO_6) coordination, respectively.[40−42] The presence of a high concentration of pentahedrally coordinated aluminum is a direct consequence of the high quantity of

(39) Liu, Q.; Wang, A. Q.; Wang, X. D.; Zhang, T. *Microporous Mesoporous Mater.* **2007**, *100*, 1.
(40) Stebbins, J. F. In *Handbook of Physical Constants*; Ahrens, T. J., Ed.; American Geophysical Union: Washington DC, 1995; Vol. 2.
(41) Akitt, J. W. *Prog. Nucl. Magn. Reson. Spectrosc.* **1989**, *21*, 127.
(42) McManus, J.; Ashbrook, S. E.; MacKenzie, K. J. D.; Wimperis, S. *J. Non-Cryst. Solids* **2001**, *282*, 278.

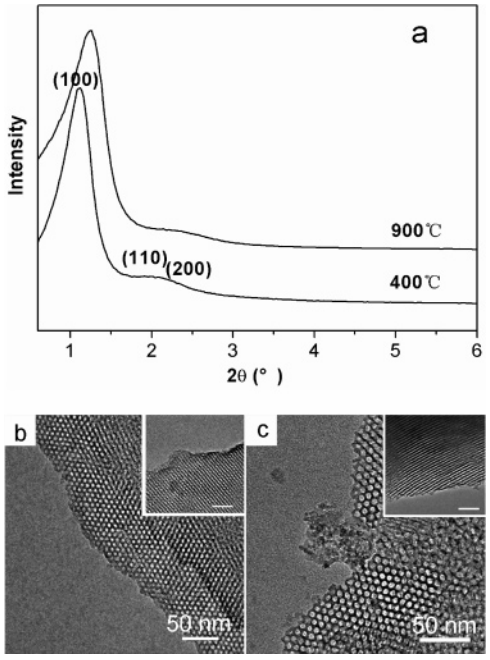

Figure 9. (a) Small-angle XRD patterns of Al-11 which using $Al(NO_3)_3$ as the precursor. TEM images of Al-11 calcined at (b) 400 and (c) 900 °C. The bars are 50 nm for insets. The bars are 50 nm for insets.

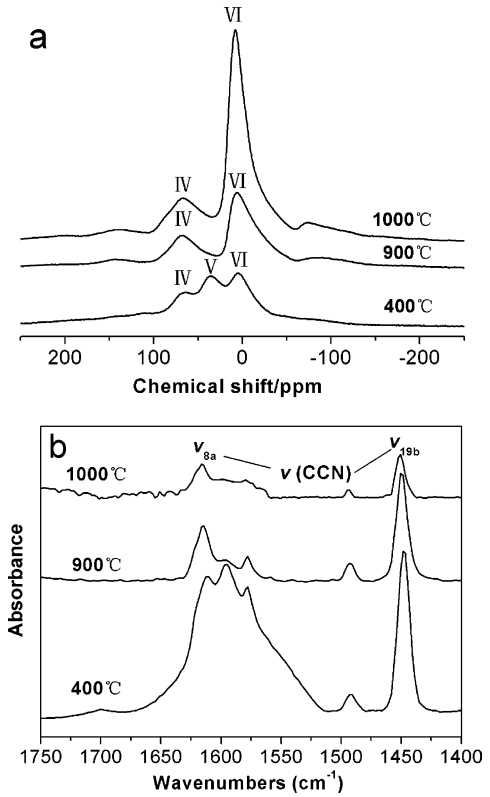

Figure 10. (a) ^{27}Al MAS NMR spectra and (b) FTIR spectra of pyridine adsorption for Al-1 at the deposition temperature of 200 °C.

defects induced by the large surface area of the network.[43] Nevertheless, in the 900 and 1000 °C calcined samples no pentahedrally coordinated aluminum is detected, whereas the amounts of tetrahedrally and octahedrally coordinated aluminum increase, which is strong evidence for the existence of the γ-alumina phase and suggests that most of the product is in crystalline form and that these nano domains are homogeneous.[17] To test the surface acidity of sample Al-1, FTIR pyridine adsorption measurements are performed. As shown in part b of Figure 10, the IR spectra of adsorbed pyridine display characteristic absorption bands at 1620 and 1450 cm^{-1} corresponding to the υ_{8a} and υ_{19b} modes of the ring-breathing vibrations υ(CCN) of pyridine, respectively, indicating pyridine adsorption via hydrogen-bonding with the surface OH groups and the nitrogen-lone-pair electrons interacting with the coordinatively unsaturated Al^{3+} ions in octahedral and tetrahedral coordination (Lewis acid sites).[44−46] The amount of absorbed pyridine on Lewis acid sites is estimated by integration of the band (υ_{19b} mode) around 1450 cm^{-1}. The numbers of Lewis acid sites calculated for Al-1 calcined at different temperatures are very large and decrease gradually with the calcined temperatures elevated (Table S2 in the Supporting Information).

Table 2. Activities of Supported Ruthenium Catalysts (2 wt % Ruthenium) in Hydrogenation of Acetone, Glucose, and Cellobiose[a]

	Conversion Rate (mol/mol·ruthenium·h)				rate ratio
catalyst	acetone[b]	glucose	cellobiose	glucose + cellobiose[c]	(glucose to cellobiose)
ruthenium/meso-Al_2O_3	4207	173	54	90 (glucose) + 9 (cellobiose)	3.2 (10.0)[d]
ruthenium/commercial-Al_2O_3	4208	510	492	372 (glucose) + 100 (cellobiose)	1.0 (3.7)[d]

[a] Reaction conditions: 120 °C, 4 MPa H_2, 0.01 mmol ruthenium, 30 min reaction time, 17.2 mmol acetone, 5.6 mmol glucose or cellobiose. [b] 15 min reaction time. [c] 5.6 mmol glucose + 5.6 mmol cellobiose. [d] Data in the parentheses are obtained from hydrogenation of an equimolar mixture of glucose and cellobiose.

These well-ordered mesoporous aluminas are examined as catalyst supports in the hydrogenation of acetone, D-glucose, and D-(+)-cellobiose with different molecular sizes as test reactions. These carbonyl compounds possess different molecular sizes of 0.38, 0.65, and 1.2 nm, respectively, which are chosen to probe the pore-size effects of the mesoporous Al_2O_3 supports. Table 2 shows the representative results of ruthenium supported on mesoporous γ-alumina (Al-11) with controlled pore sizes of 3.6 nm (ruthenium/meso-Al_2O_3) and for comparison, on commercial γ-alumina (ruthenium/commercial-Al_2O_3) with larger pore sizes of predominantly 10 nm (Figure S10 in the Supporting Information). TEM characterization (Figure 11) shows that ruthenium particles on the two Al_2O_3 supports possess narrow unimodal size distributions with similar mean diameters of 3.0 and 2.9 nm, respectively, indicating similar ruthenium dispersions. On these two catalysts, acetone, glucose, and cellobiose are hydrogenated exclusively to their corresponding alcohols, 2-propanol, sorbitol, and 3-β-D-glucopyranosyl-D-glucitol respectively at 120 °C and 4 MPa H_2.

The conversion rates (normalized by the total ruthenium content) depend largely on the size of the support pores and reactants. The two catalysts are active and give identical rates (4207−4208 mol/mol·ruthenium·h, Table 2) for the hydrogenation of acetone, the smallest molecule chosen, demonstrating their same intrinsic hydrogenation activities. For glucose and cellobiose, their hydrogenation rates on ruthenium/meso-Al_2O_3

(43) Chupas, P. J.; Grey, C. P. *J. Catal.* **2004**, *224*, 69.
(44) Abbattista, F.; Delmastro, S.; Gozzelino, G.; Mazza, D.; Vallino, M.; Busca, G.; Lorenzelli, V.; Ramis, G. *J. Catal.* **1989**, *117*, 42.
(45) Kawai, T.; Jiang, K. M.; Ishikawa, T. *J. Catal.* **1996**, *159*, 288.
(46) Layman, K. A.; Ivey, M. M.; Hemminger, J. C. *J. Phys. Chem. B* **2003**, *107*, 8538.

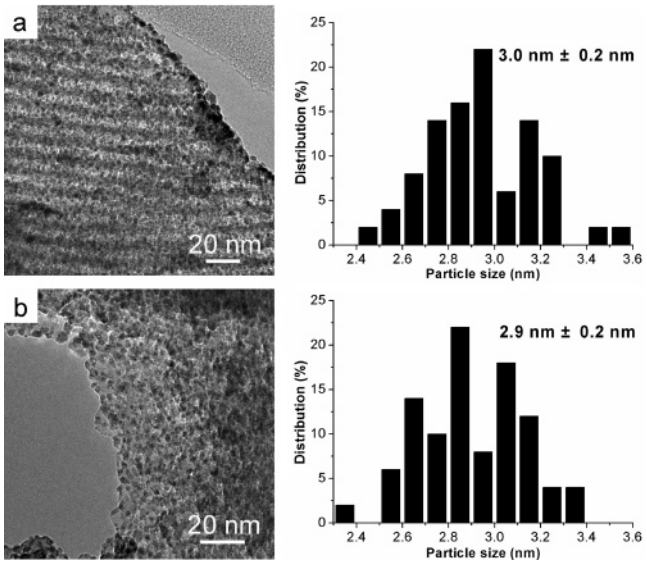

Figure 11. TEM images and histograms of ruthenium particle size distribution of (a) ruthenium/meso-alumina catalyst and (b) ruthenium/commercial alumina catalyst.

are 173 and 54 mol/mol·ruthenium·h, respectively. In contrast, glucose and cellobiose convert at similar rates (510 vs 492 mol/mol·ruthenium·h) on ruthenium/commercial-Al_2O_3, which are approximately three and nine times greater than those on ruthenium/meso-Al_2O_3, respectively. Such differences in the conversion rates are apparently related to the effects of steric hindrance, imposed by the molecular sizes of the reactants relative to the pore sizes of the Al_2O_3 supports, on the diffusion and accessibility of the reactants to the ruthenium domains confined inside the pores. Taken together, these results reflect the features of reactant size selectivity of the ordered mesoporous Al_2O_3 supports, which are further confirmed by hydrogenation of an equimolar mixture of glucose and cellobiose. As shown in Table 2, the coexistence of glucose and cellobiose leads to a more preferential reaction of glucose over cellobiose on ruthenium/meso-Al_2O_3, and their conversion rates are different by an order of magnitude, much greater than that on ruthenium/commercial-Al_2O_3 (being 3.7) under the same conditions and also than that obtained with individual reactants on ruthenium/meso-Al_2O_3 (being 3.2). This observed size selectivity of the ordered mesoporous aluminas, together with their controllable pore sizes and high thermal stability, provides their potential applications in shape-selective catalysis.

Conclusions

We have demonstrated the systematic fabrication of highly ordered mesoporous amorphous and/or crystalline γ-aluminas with high thermal stability by a facile synthesis method. The simplicity, versatility, and reproducibility of this synthetic approach will facilitate the development of new mesoporous materials. The mesostructures are stable at a temperature as high as 1000 °C, which is an excellent advantage in high-temperature catalytic reactions. Moreover, tunable pore sizes from 3 to 7 nm (Table S1 in the Supporting Information) make the shape-selective catalysis become possible.[47] Strong Lewis acidity, provided by aluminum atoms in tetrahedral and octahedral coordination sites, proves these ordered mesoporous aluminas to be ideal supports for heterogeneous catalysis. Serving as catalyst supports of ruthenium in the hydrogenation reaction, these materials exhibit size selectivity for different molecules with different sizes, promising potential applications in shape-selective catalysis.

Acknowledgment. This work was supported by the MOST of China (2006CB601104), NSFC (Grants 20221101, 20610068, and 20423005), and the Founder Foundation of PKU.

Supporting Information Available: Small- and wide-angle XRD patterns of Al-1 calcined at 1100 °C, additional TEM images of Al-1 calcined at 400 °C prepared in two batches, FTIR spectra of the pure CA and the as-synthesized samples prepared with different CA/Al^{3+} ratios, small-angle XRD patterns of samples calcined at 400 °C with different CA/Al^{3+} ratios using aluminum iso-propoxide and hydrous aluminum nitrate as the precursor, nitrogen adsorption−desorption isotherms combined with corresponding pore-size distribution curves deduced from the desorption branches, physicochemical properties of ordered mesoporous alumina, band position and the number of Lewis acid sites of Al-1. This material is available free of charge via the Internet at http://pubs.acs.org.

JA0764308

(47) (a) Blasco, T.; Corma, A.; Navarro, M. T.; Pérez, Pariente, J. *J. Catal.* **1995**, *156*, 65. (b) Corma, A.; Corell, C.; Pérez, Pariente, J.; Guil, J. M.; Guil Lopez, R.; Ncolopoulos, S.; Calbet, J. G.; Vallet, Regi, M. *Zeolites* **1996**, *16*, 7.